Angiogenesis (2014) 17:119–128
DOI 10.1007/s10456-013-9382-5

ORIGINAL PAPER

Dendritic cells regulate angiogenesis associated with liver fibrogenesis

Sandra M. Blois · Flavia Piccioni · Nancy Freitag · Irene Tirado-González · Petra Moschansky · Rodrigo Lloyd · Karin Hensel-Wiegel · Matthias Rose · Mariana G. Garcia · Laura D. Alaniz · Guillermo Mazzolini

Received: 30 April 2013 / Accepted: 2 September 2013 / Published online: 26 September 2013

Abstract During liver fibrogenesis the immune response and angiogenesis process are fine-tuned resulting in activation of hepatic stellate cells that produce an excess of extracellular matrix proteins. Dendritic cells (DC) play a central role modulating the liver immunity and have recently been implicated to favour fibrosis regression; although their ability to influence the development of fibrogenesis is unknown. Therefore, we explored whether the depletion of DC during early stages of liver injury has an impact in the development of fibrogenesis. Using the CD11c.DTR transgenic mice, DC were depleted in two experimental models of fibrosis in vivo. The effect of anti-angiogenic therapy was tested during early stages of liver fibrogenesis. DC depletion accelerates the development of fibrosis and as a consequence, the angiogenesis process is boosted. We observed up-regulation of pro-angiogenic factors together with an enhanced vascular endothelial growth factor (VEGF) bioavailability, mainly evidenced by the decrease of anti-angiogenic VEGF receptor 1 (also known as sFlt-1) levels. Interestingly, fibrogenesis process enhanced the expression of Flt-1 on hepatic DC and administration of sFlt-1 was sufficient to abrogate the acceleration of fibrogenesis upon DC depletion. Thus, DC emerge as novel players during the development of liver fibrosis regulating the angiogenesis process and thereby influencing fibrogenesis.

Keywords Dendritic cells · Angiogenesis · Liver fibrogenesis · sFlt-1

Flavia Piccioni and Nancy Freitag have contributed equally to this work.

Electronic supplementary material The online version of this article (doi:10.1007/s10456-013-9382-5) contains supplementary material, which is available to authorized users.

S. M. Blois (✉) · N. Freitag · I. Tirado-González · P. Moschansky · M. Rose
Charité Center 12 Internal Medicine and Dermatology, Reproductive Medicine Research Group, Universitätsmedizin Berlin, Berlin, Germany
e-mail: sandra.blois@charite.de

F. Piccioni · R. Lloyd · M. G. Garcia · L. D. Alaniz · G. Mazzolini (✉)
Gene Therapy Laboratory, Facultad de Ciencias Biomédicas, Universidad Austral, Av. Presidente Perón 1500, B1629ODT Derqui-Pilar, Buenos Aires, Argentina
e-mail: gmazzoli@cas.austral.edu.ar

F. Piccioni · R. Lloyd · M. G. Garcia · L. D. Alaniz · G. Mazzolini
CONICET (Consejo Nacional de Investigaciones Científicas y Técnicas), Buenos Aires, Argentina

K. Hensel-Wiegel
Zentrallabor Campus Virchow-Klinikum, Universitätsmedizin Berlin, Berlin, Germany

Introduction

Liver fibrosis is a wound healing process that occurs in response to a number of hepatic diseases such as alcohol abuse and chronic viral hepatitis, while less frequent causes include autoimmune hepatitis, drugs, biliary and metabolic diseases [1, 2]. As a result of liver fibrosis, formation of new blood vessels, sinusoidal remodeling and changes in extracellular matrix (ECM) composition and organization were observed. In this scenario, activated hepatic stellate cells (HSC) play a key role as the major collagen-ECM-producing cells [2]. The accumulation of ECM components and advanced fibrosis may result in cirrhosis, hepatic failure, and increased portal pressure often leading to liver transplantation [1]. Although the mechanisms leading to HSC activation are increasingly

known, the contribution of different resident immune cells during the fibrogenic processes is less explored [3].

During the last years a number of studies have attempted to evaluate the role of diverse immune subsets, such as Kupffer cells, natural killer (NK) cells, lymphocytes and dendritic cells (DC), in the regulation of inflammatory microenvironments in experimental models of liver fibrosis [4–8]. DC are the most potent specialized antigen presenting cells and the physiologic initiators of cellular immune responses [9]. Bridging the innate and adaptive immune systems, DC have the ability to regulate inflammation through their capacity to release cytokines and chemokines [10]. Upon maturation DC increase their expression of molecules involved in $CD4^+$ T cell differentiation towards the Th1 pro-inflammatory phenotype and in DC trafficking towards secondary lymphoid organs [11]. On the contrary, immature DC have the ability to induce a tolerogenic response [12]. It has been observed in hepatitis C patients that progression towards chronic disease and fibrosis is related, at least in part, to an immunosuppressive microenvironment induced by HCV chronic infection where DC play a key role [13]. Conolly et al. [14] recently showed that hepatic DC contribute to advanced stages of fibrosis through the secretion of TNF-α. In addition, it has recently been observed that DC favour fibrosis regression and that this effect is due to MMP-9 production [15].

In cirrhotic livers, the fibrous tissue is highly vascularized suggesting that angiogenic factors may be involved in the pathogenesis of the disease. It has been observed that pro-angiogenic factors, such as vascular endothelial growth factor (VEGF), expressed by hepatocytes contribute to fibrogenesis in different experimental models [16–20]. Interestingly, DC may produce diverse pro- and anti-angiogenic factors depending on their activation status and cytokine microenvironment [21, 22]. However, their potential role as angiogenesis regulator during liver fibrogenesis is poorly understood. In the present study, we evaluated the role of DC during early phases of liver fibrogenesis in vivo, providing evidences that overproduction of angiogenic growth factors generated after DC depletion may play an important role in the pathogenesis of the disease. In addition, we highlighted the role of DC in regulating VEGF bioavailability by secreting sFlt-1 and showed that their depletion accelerates the process of fibrogenesis.

Methods

Liver fibrosis model

Seven- to eight-week C57BL/6 CD11c.DTR male mice, which express the diphteria toxin receptor (DTR) under the control of the CD11c promoter as described by Jung et al. [23], were purchased from Jaxmice (Charles River, Germany) and maintained in our animal facility with a 12L/12D cycle with free access to food and water. Mice were injected intraperitoneally (i.p.) with thioacetamide (TAA, Sigma Aldrich, Germany) at 0.2 mg/g body weight (BW) or saline used as control three times/week for a period of 4 weeks. As a second model carbon tetrachloride (CCl4)-induced liver damage was used [24]. Mice were treated with i.p. injection twice/week with 0.75 ml CCl4/kg of BW (2:5 v/v in mineral oil) for 4 weeks. Small pieces of each lobe were snap frozen in liquid nitrogen, embedded in optimal cutting temperature compound, and stored at −80 °C until analysis, or fixed in 10 % phosphate saline-buffered neutral formalin. Procedures that involved mice were approved by the state authority for Animal Use in Research and Education and were conducted in strict accordance with guidelines for the care and use of laboratory research animals promulgated by the Medicine University of Berlin and Austral University.

Expansion and depletion of dendritic cells (DC)

In order to expand DC during early fibrosis, CD11c.DTR male mice (n = 5–7) were treated with one daily i.p. injection of human recombinant Flt-3L (500 ng/g BW in PBS, BioxCell) for 7 consecutive days during the third week of TAA treatment. For the depletion of DC, CD11c.DTR mice were injected only once with Diphtheria toxin (DT, 4 ng/g BW in PBS) during the third week of the TAA- or CCl4-induced fibrosis.

Soluble VEGF receptor 1 chimera (sFlt-1-Fc) treatment

DC depleted mice were injected with a single intravenous (i.v.) injection of sFlt-1/Fc (130 pg/day, R&D Systems) for 7 consecutive days during the third week of TAA treatment.

Enzyme-linked immunosorbent assay (ELISA)

Serum samples were tested in competitive ELISA using kits obtained from R&D Systems to quantify VEGF (Duoset mouse VEGF, Cat DY493) following the manufacturer's recommendations. The quantification of Flt-1 serum levels was performed using the Mouse Flt-1 Quantikine Immunoassay (R&D Systems, Cat MVR100) following the manufacturer's instructions. Endoglin levels in serum were determined using mouse Endoglin/CD105 DuoSet from R&D Systems (Cat DY1320) following the manufacturer's recommendations.

Adoptive transferred bone marrow-derived DC (BM-DC)

Bone marrow-derived DC were obtained as previously described [25]. Briefly, bone marrow cells (10^6 cells/ml) were plated into 6-well plates and cultured for up to 7 days with recombinant murine granulocyte–macrophage colony-stimulating factor (GM-CSF, 20 ng/ml, Peprotech). The culture medium was half-renewed every 3 days. At day 7 of culture, BM-DC were stimulated to mature by adding 1 μg/ml lipopolysaccharides (LPS, Sigma-Aldrich) for 18 h.

Cytokine determination by cytometric bead arrays (CBA)

Cytokines were analyzed in serum using cytometric bead arrays (CBA) as described previously [26]. Briefly, serum samples were stored at −80 °C until cytokine determination. TNF-α, IL-6, MCP-1 and IL-10 were detected simultaneously using the mouse inflammation cytokine CBA kit (BD Bioscience, San Diego, CA). Briefly, 50 μl of each sample was mixed with 50 μl of mixed capture beads and 50 μl of the mouse inflammation PE detection reagent consisting of PE-conjugated anti-mouse TNF-α, IL-6, MCP-1 and IL-10. The samples were incubated at room temperature for 2 h in the dark. After incubation with the PE detection reagent, the samples were washed once and resuspended in 300 μl of wash buffer before acquisition on the FACScalibur (Becton–Dickinson). Data were analyzed using FCAP array software (BD Bioscience).

Angiogenesis array

The expression profile of angiogenesis-related proteins in the livers from DC depleted and TAA treated mice were analyzed using the Proteome Profiler™ from (R&D systems, cat. ARY015) following the manufacturer's instructions.

RNA isolation and quantitative PCR analysis

Total RNA was extracted from liver tissue using the Nucleospin RNA/protein isolation kit (Macherey–Nagel). After DNase digestion (Invitrogen), cDNA was generated using random primers (Invitrogen). Real-time qPCR was performed on the TaqMan 7500 System (Aplied Biosystems). For each reaction, 1 μl cDNA, synthesized from 1 μg RNA in 25 μl, was used in a total volume of 11 μl containing 6.25 μl of Power SYBR Green PCR mastermix (Applied Biosystems), 3.75 μl DEPC water and 450 nM of the appropriate forward and reverse primers. The following primers were used: CXCL12 (forward primer: 5′-GAGA GCCACATCGCCAGAG-3′, reverse primer: 5′-TTTCG GGTCAATGCACACTTG-3′). The PCR profile was as follows: 2 min 50 °C, 10 min at 95 °C, followed by 40 cycles of 15 s at 95 °C and 60 s at 60 °C. Subsequently, a melting curve analysis was performed which consisted of 70 cycles of 10 s with a temperature increment of 0.5 °C/cycle starting at 60 °C. The relative expression was calculated according to the equation Rel. Exp (RE) $= 2^{-\Delta Ct}$.

Histology analysis

Paraffin embedded liver samples were cut in 4 μm thick sections and stained with haematoxylin-eosin (H&E), Masson's trichrome and Sirius red according to standard procedures. Analyses were performed in a blinded fashion.

Liver enzymes

Enzyme levels of aspartate aminotransferase (AST), alanine aminotransferase (ALT) and alkaline phosphatase (ALP) were determined in serum samples obtained before and after DC depletion during the TAA treatment. Serum samples of experimental animals were analyzed using routine laboratory techniques HITACHI (Roche) auto analyser equipped with a Cobas 800 system software.

Immunofluorescence analysis

Eight micrometer cryosections were blocked and incubated with different primary antibodies: anti- α-smooth muscle actin (SMA, Sigma Aldrich), anti-endoglin (Santa Cruz Biotechnology) or anti-vascular cell adhesion molecule-1 (VCAM-1, BD Bioscience). Rhodamine-labeled secondary antibodies (Jackson Immuno-Research) were used followed by 4′,6-diamidino-2-phenylindole (DAPI). Sections were analyzed using a confocal laser scanning microscope (cLSM 510, Carl Zeiss, Germany).

FACS analysis

Isolated hepatic DC (hDC) were resuspended in PBS, 1 % Bovine serum albumin (BSA) solution and pre-incubation with 1 % anti-mouse CD16/CD32 monoclonal antibody and 10 % mouse serum was carried out to avoid unspecific staining via Fc-receptor. Then hDC were incubated for 30 min at 4 °C with FITC-conjugated rat anti mouse CD11c (clone HL3, BD Biosciences), PE-anti mouse IA^b (clone M5/114.15.2, BD Biosciences) and PerCP-anti mouse CD86 [clone 2331 (FUN-1), BD Biosciences]. After washing the acquisition was performed using the FACS Calibur system (BD Biosciences). Data were analyzed using FlowJo software.

Statistics

Data were analyzed with Student's *t* test or the analysis of variance with Bonferroni correction for multiple comparisons between groups. Data are expressed as mean ± SEM. Statistical significance was designated as $p < 0.05$.

Results

DC depletion accelerates the development of liver fibrosis

To investigate the role of DC during liver fibrogenesis, we used two experimental strategies. The first one involved the transgenic CD11c.DTR mice which allow conditional ablation of DC by a single injection of diphtheria toxin (DT) and the second strategy consisted in expansion of DC by administration of Flt-3L for 7 consecutive days. In order to identify the beginning of TAA-induced fibrogenesis process, we evaluated collagen deposition using the Sirius red staining after 1, 2 and 3 weeks of treatment (Fig. S1). Histological analysis revealed a visible collagen deposition after 3 weeks of TAA treatment. Therefore, we have chosen this period (3wk) to deplete or expand DC in the liver (Fig. 1a), whereas the TAA administration continues for 4wk. As shown in Fig. 1b, the liver surface showed a gross fibrotic appearance upon 4wk TAA treatment but no macroscopic differences could be observed when comparing the different groups. However, histological examination confirmed that the livers of DC depleted TAA treated mice exhibited a more extensive collagen deposition and pseudo lobular formation indicative of bridging fibrosis (F3) than DC expanded or TAA treated mice (F1) (Fig. 1c,

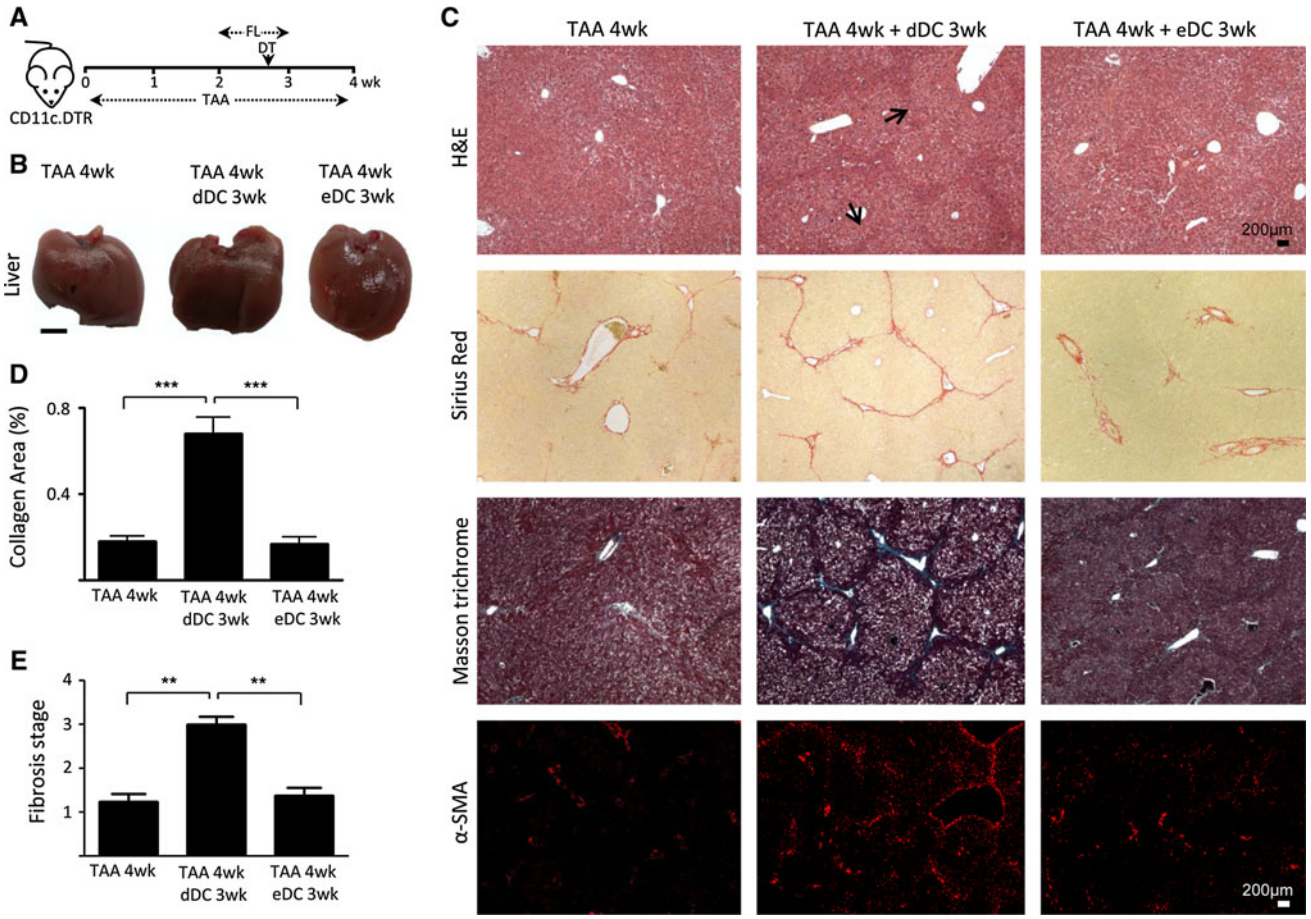

Fig. 1 Depletion of DC accelerate hepatic fibrogenesis. **a** Experimental design: CD11c-DTR mice were injected i.p. with thioacetamide (TAA) and diphtheria toxin (DT; 4 ng/g BW) or daily with 10 µg Flt-3L for 7 days, as described in "Methods". **b** The liver surface contour of all treated mice was markedly heterogeneous. *Scale bar* 0.5 cm. **c** *H&E*, *Sirius red*, *Masson's trichrome* and *α-SMA* examination of the livers of treated mice. Original magnification ×5. *Sirius red* staining of liver tissue from TAA 4wk + dDC 3wk revealed extensive collagen deposition and pseudolobular formation, indicative of bridging fibrosis. *Scale bar* 200 µm. **d** Morphometric quantification of *Sirius red* stained area showing a significant increment of the fibrotic process in DC depleted mice. **e** Histological staging of liver fibrosis. In **d**, **e**, significant differences are noted as $^{**}p < 0.01$ and $^{***}p < 0.001$ as analyzed by one-way ANOVA followed by Bonferroni test

Table 1 Changes in serum alanine aminotransferase (ALT), aspartate aminotransferase (AST) and alkaline phosphatase (ALP) activities in DC depleted mice treated with TAA

Groups	ALT (U/l)		AST (U/l)		ALP (U(l)	
TAA 4wk	301.8 ± 24.4^{b}	323.6 ± 45.5^{a}	183.3 ± 24.1^{b}	213.5 ± 8.4^{a}	79.7 ± 10.5^{b}	91.4 ± 4.6^{a}
TAA 4wk dDC 3wk	291.3 ± 26.1^{b}	535.6 ± 25.8^{a}**	206.5 ± 10.7^{b}	295.8 ± 12.3^{a}*	74.2 ± 7.9^{b}	161.8 ± 4.3^{a}**

Values are mean ± S.E.M. with n = 5. Column values with different superscript letters represent liver analysis performed b = before and a = after DC depletion over the TAA treatment. Significant differences are noted as * $p < 0.05$ and ** $p < 0.01$ as analyzed by Student's *t* test

d). As shown in Table 1, liver enzymes (ALT, AST and ALP) were significantly increased in the liver of the DC depleted mice as compared to only TAA treated mice. DC depletion was also associated with increased activated HSC in comparison with TAA treatment alone, as depicted by α-SMA expression (Fig. 1c). In order to quantify liver content of collagen, the ECM protein most abundantly accumulated in fibrous septae, tissue sections from 4wk TAA-treated animals were Sirius red stained and morphometric analysis was thereafter performed. A significant increment in the Sirius red positive area was found in DC depleted mice when compared to DC non-depleted or expanded mice. Similar results were observed using the CCl4 model (Fig. S2).

DC ablation influences the cytokine environment during liver fibrogenesis

To define the mechanism through which DC influence fibrogenesis, we assessed the phenotype of $CD11c^{+}$ cells isolated from liver tissue of TAA and TAA-dDC treated mice. As shown in Fig. 2a, the expansion of DC during the process of fibrogenesis is delayed in the TAA-dDC mice, evidenced by low percentage of nonparenchymal $CD11c^{+}$ cells isolated from the liver. In particular, $CD11c^{+}$ DC from TAA-dDC liver exhibited immature phenotype when compared to TAA isolated DC (Fig. 2a). In addition, inflammatory cytokines (e.g. TNF-α, IL-6 and MCP-1) were up-regulated immediately after DC depletion on week 3 (Fig. 2b). However, TNF-α and IL-6 were restored to control levels during the 4-week of the TAA treatment (Fig. 2c). The down-regulation from TNF-α and IL-6 was accompanied by a significant decrease of IL-10 (Fig. 2c).

Angiogenesis is boosted upon DC ablation

Knowing that DC are able to influence angiogenesis process during both physiological and pathological process [27–30], we examined the expression of endothelial markers in liver upon DC depletion. Compared to TAA mice, in which discrete endoglin and VCAM-1 expression was observed (Fig. 3a, left panel), activation of endothelial cells was evidenced by a markedly increased staining of both markers in TAA-dDC livers (Fig. 3a, b). However, no difference was observed in sEndoglin levels between TAA and TAA-dDC treated mice (Fig. 3c). DC ablation during fibrogenesis increased the bioavailability of VEGF, evidenced by the significant reduction of anti-angiogenic sFlt-1 (Fig. 3d). In addition, mRNA levels of CXCL12 were significantly increased upon DC depletion during fibrogenesis, reflecting the increased bioavailability of VEGF in the liver as reported previously [31] (Fig. 3e). To directly define the angiogenic status upon DC depletion, we assessed the protein profile in the whole liver. As shown in Fig. 3f, pro-angiogenic proteins such as angiogenin (ANG), tissue factor (TF), heparin-binding epidermal growth factor (HB-EGF) and serprin E1 (PAI-1) were increased upon DC ablation during fibrogenesis. In addition, anti-angiogenic factors e.g. pigment epidermal derived factor (PEDF), thrombospondin-2 (TSP-2) and pentraxin-3 (PTX-3) and proteins involved in liver regeneration such as fibroblast growth factor-2 (FGF-2), hepatocyte growth factor (HGF), IGF binding protein-1 and -9 (IGFBP-1 and -9) were down-regulated by DC depletion (Fig. 3g).

DC regulate angiogenesis associated with liver fibrogenesis via Flt-1

To further establish the role of hepatic DC in regulating the bioavailability of VEGF, we assessed Flt-1 expression during the initiation of fibrogenesis at 3wk in DC depleted TAA treated mice. Compared to TAA treated mice, in which prominent staining around blood vessels was observed after fibrosis induction, Flt-1 expression was absent in DC depleted TAA treated mice Fig. 4a. In addition, the process of liver fibrogenesis results in an increased Flt-1 expression by the non-parenchymal $CD11c^{+}$ cells isolated from the liver (Fig. 4b). Moreover, LPS stimulated liver $CD11c^{+}$ cells exhibited a higher Flt-1 expression compared with non-stimulated DC, suggesting that mature hepatic DC are able to regulate VEGF bioavailability in a more efficient manner. To provide direct evidence that Flt-1 is able to prevent the exacerbation of liver fibrogenesis upon DC depletion, we treated CD11c.DTR mice with sFlt-1 during the period where DC were absent, as shown in Fig. 4c. A sFlt-1/Fc-mediated VEGF bioavailability reduction strategy [32] was chosen

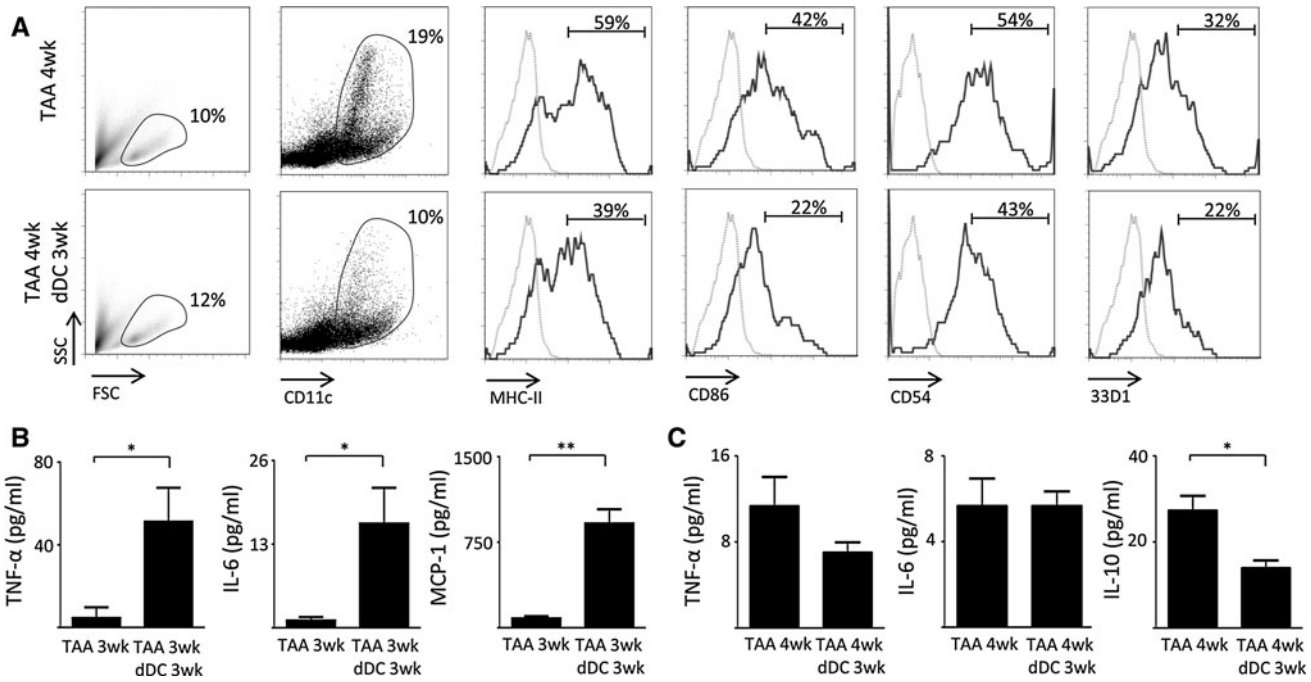

Fig. 2 DC ablation transiently changed cytokine microenvironment during liver fibrogenesis. **a** Liver DC characterization by FACS. Inserted grey depicts the isotype control. Results correspond to at least three independent experiments using four to six animals/group. **b** Cytometric Beads Assay (CBA) determination of TNF-α, IL-6 and MCP-1 (pg/ml) concentration in serum from 3wk treated mice. **c** Cytometric Beads Assay (CBA) determination of TNF-α, IL-6 and IL-10 (pg/ml) concentration in serum from 4wk TAA treated mice. All treatments were performed in triplicate in at least three independent experiments. In all figures, significant differences are noted as $*p < 0.05$ and $**p < 0.01$ as analyzed by Student's t test

over the adenovirus-mediated sFlt-1 because of its unacceptable hepatotoxicity [33]. As depicted in Fig. 4d, e, DC depleted-sFlt-1 TAA treated mice had similar deposition of collagen to the observed in TAA treated mice. This data suggests that sFlt-1 is sufficient to reduce liver fibrosis upon DC depletion.

Adoptive transfer of bone marrow-derived DC (BM-DC) ameliorates fibrogenesis

To assess whether immature or mature DC could prevent the TAA-induced fibrogenesis, we adoptively transferred immature (iBM-DC) and mature (mBM-DC) bone marrow-derived DC stimulated with LPS during the third week of TAA administration. As shown in Fig. S3, mice that received either immature or mature DC depicted a discrete collagen deposition compared to TAA group, as evidenced by the Sirius red staining. In order to address whether either the number of myofibroblasts in fibrous septae and/or the activation state of myofibroblasts might be affected by mBM-DC adoptive transfer, liver tissue obtained from 4 weeks TAA-treated mice was immunostained with α-SMA. A significant reduction in the α-SMA$^+$ immunostained area was found in both iBM-DC and mBM-DC treated mice when compared to TAA mice (Fig. S3). Next, we analyzed Flt-1 expression in iBM-DC and mBM-DC cells used in this experiment. As depicted in Fig. S3, similar Flt-1 expression was observed in both iBM-DC and mBM-DC, suggesting that BM-DC cells have a similar ability to regulate the bioavailability of VEGF and therefore to reduce liver fibrosis.

Discussion

Angiogenesis and disruption of vascular architecture have been linked to progression of liver fibrogenesis. Indeed, a recent study in mice showed that administration of an angiostatic chemokine (e.g. CXCL9) attenuates angiogenesis and experimental liver fibrosis in vivo [34]. Although DC exert an important role during angiogenesis in different physiopathological settings, e.g. in cancer [27–30], their role as angiogenesis regulators during liver fibrosis is not yet fully understood. Here, we showed that ablation of DC resulted in acceleration of liver fibrosis in vivo. Changes in the hepatic cytokine environment and a dominant immature DC phenotype characterize DC depleted livers, while non-treated mice showed predominantly an activated DC phenotype. In addition, angiogenesis seems to be boosted upon DC ablation due to, at least in part, a reduction in sFlt-1 levels which enhances VEGF bioavailability. Experimental angiotatic strategy (sFlt-1/Fc) was able to

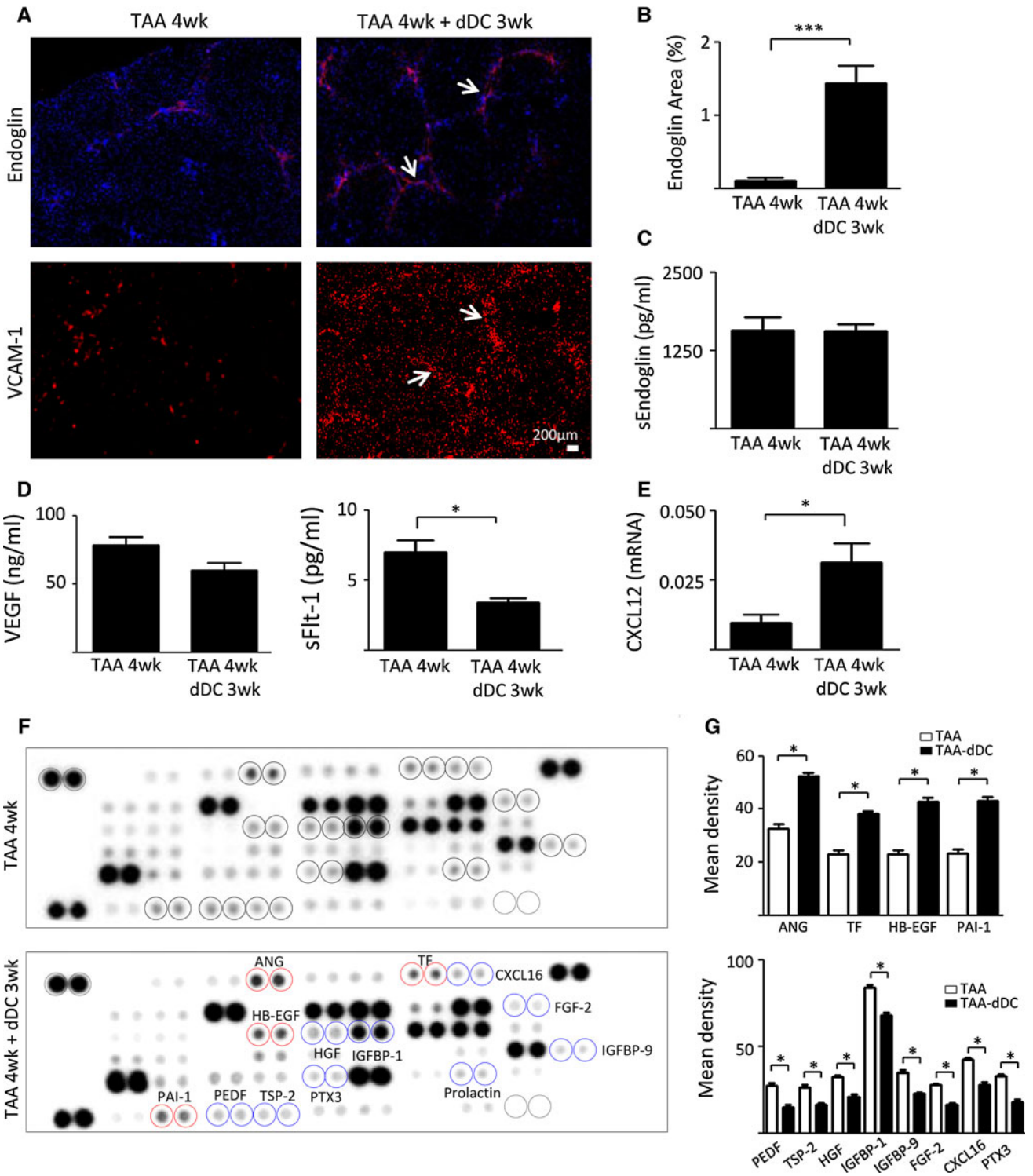

Fig. 3 Effect of DC depletion during fibrogenesis in the angiogenesis process. **a** Endoglin and VCAM-1 liver expression analyzed by IF. **b** *Graphs* show the percentage of liver area positive for endoglin. **c** sEndoglin analysis in serum by ELISA. **d** VEGF and sFtl-1 determination in serum by ELISA. **e** CXCL12 mRNA levels analyzed by qPCR. Results correspond to at least three independent experiments using five to seven animals/group. **f** Angiogenesis array in liver tissue lysates from TAA and depleted DC-TAA treated mice. *Red encircled proteins* denote up-regulated, whereas *blue encircled proteins* shown down-regulated in TAA-dDC mice. In all figures, significant differences are noted as $*p < 0.05$ and $***p < 0.001$ as analyzed by one-way analysis of variance (ANOVA) with Bonferroni's post test

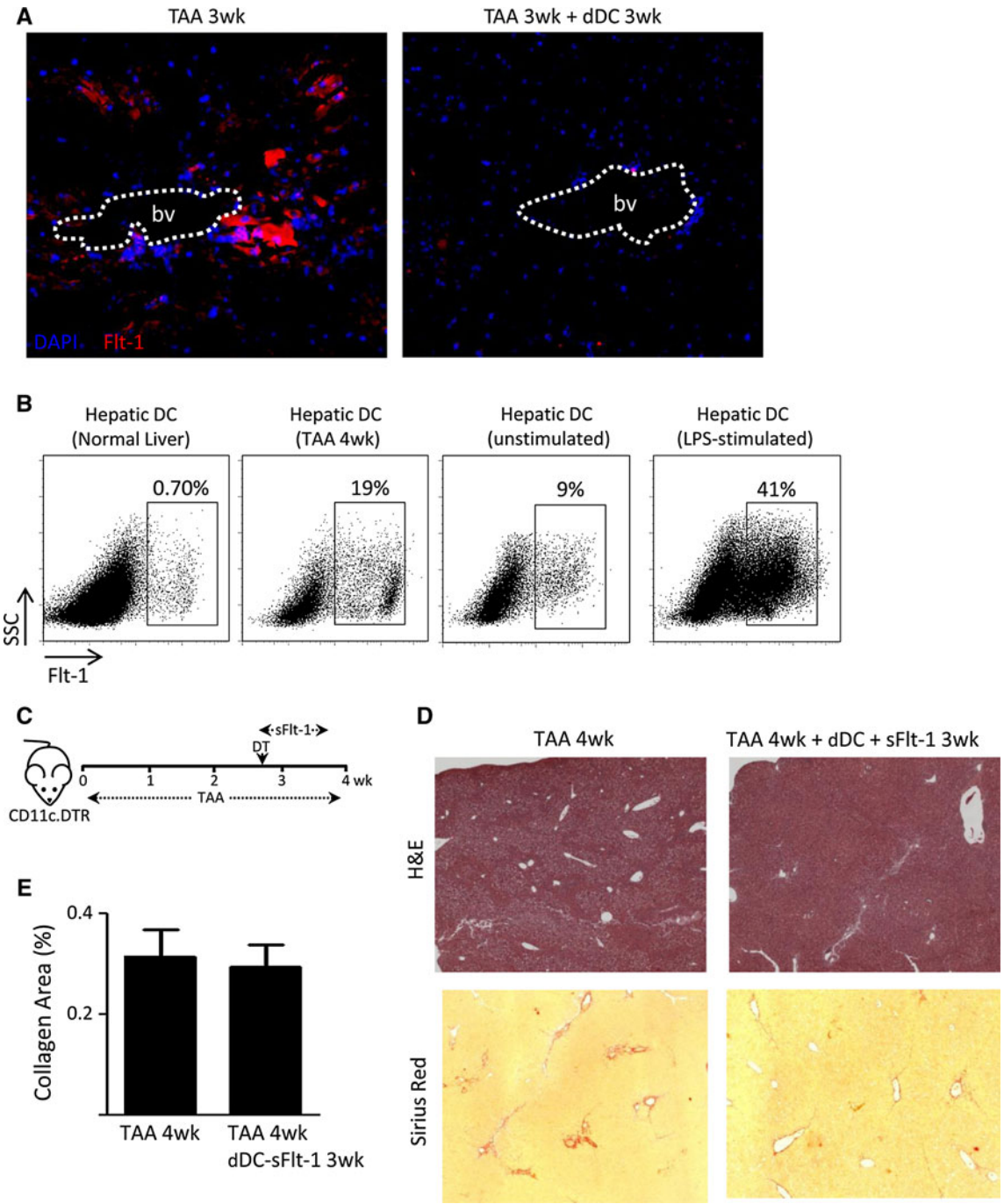

Fig. 4 Flt-1 is sufficient to ameliorate liver fibrosis in vivo upon DC depletion. **a** Flt-1 liver expression analyzed by IF. **b** Flt-1 expression on hepatic DC by FACS. Results correspond to at least three independent experiments using 2–4 animals/treatment. **c** Experimental design: CD11c-DTR mice were injected i.p. with thioacetamide (TAA), diphtheria toxin (DT; 4 ng/g BW) and soluble VEGF receptor 1 chimera (sFlt-1-Fc; 130 pg/day for 7 days), as described in "Methods". **d** H&E and *Sirius Red* examination of the livers in TAA, DC depleted and sFlt-1 treated mice. Original magnification ×5. *Sirius red* staining of liver tissue from TAA 4wk + dDC + sFlt-1 3wk revealed similar collagen deposition as TAA 4wk treated mice. *Scale bar* 200 μm. **e** *Graphs* show the percentage of liver area positive for *Sirius red*

abrogate hepatic fibrosis induced by DC depletion. Interestingly, experimental fibrosis increases the expression of Flt-1 on hepatic DC when compared with DC derived from a healthy liver. Collectively, this study describes a key role for hepatic DC during angiogenesis associated with liver fibrogenesis.

We demonstrated that the presence of DC exerts a protective effect during the development of experimental

liver fibrosis. Alterations of DC frequency have been found to play a role during liver fibrosis regression, due to their ability to secrete MMP-9 [15]. However, our work is the first to describe the involvement of DC during the early phase of the fibrogenic process within the liver. Indeed, DC depletion in both the TAA and CCl4 models increased the amount of collagen deposition and fibrosis degree in comparison with control non-depleted mice. Importantly, this effect was also accompanied by an increased activation of HSC, which represent the most relevant pro-fibrogenic cells in chronic liver diseases, as depicted by α-SMA expression. This is of particular importance because HSC in their activated phenotype have an active role in promoting angiogenesis which contributes to development of liver fibrosis [35, 36].

Stages of angiogenesis involve (1) dilation and increased permeability of blood vessels, which normally is stimulated by VEGF; (2) subsequent degradation of membrane basement, extracellular matrix and detachment of pericytes facilitated by factors such as Ang1, TGF-β, and MMPs; (3) angiogenic stimuli then facilitate proliferation and migration of endothelial cells, and finally, (4) stabilization of the new blood vessels occurs [37]. In this work, we showed that the sFlt-1 circulating levels were diminished upon DC depletion, reflecting an increased VEGF bioavailability, which promotes the expression of CXCL12 in the liver and the migration and retention of accessory cells during the process of angiogenesis [31]. This is of particular importance because it was observed that the CXCL12/CXCR4 pathway exerts an important role in recruitment and retention of cells of the immune system in the liver of patients with chronic HCV and HBV infection [38]. In addition, endoglin which is part of the TGF-β receptor complex was over-expressed in liver sinusoidal endothelium upon DC depletion, suggesting that TGF-β could participate in accelerated angiogenesis. Indeed, analysis of liver proteins derived from DC depleted mice exhibited a pronounced pro-angiogenic profile when compared with non-depleted TAA treated mice. Of note, DC depletion during experimental liver fibrosis promotes the down-regulation of proteins involved in liver regeneration (e.g. FGF, IGFBP-1 and -9) and also anti-angiogenic factors. Under these circumstances, angiogenesis is boosted upon DC depletion. Furthermore, we provide direct evidence that sFlt-1 is sufficient to prevent the exacerbation of liver fibrogenesis upon DC depletion. In addition, adoptive transfer of bone marrow-derived DC (BM-DC) ameliorates fibrogenesis independently of their maturation state. This result could be explained by the similar Flt-1 expression observed in both iBM-DC and mBM-DC, suggesting that both BM-DC cells have a similar ability to regulate the bioavailability of VEGF and, therefore, to reduce the amount of hepatic fibrosis.

Collectively, our results suggest that DC play a critical role during the fibrogenic process and their depletion results in accelerated collagen accumulation mainly by boosting liver angiogenesis. Moreover, this work describes novel insights on the impact of anti-angiogenic sFlt-1 in the development of experimental liver fibrogenesis and sets the stage for further evaluation of its potential therapeutic application in liver diseases associated with enhanced angiogenesis and fibrosis. From a clinical point of view, this work suggests that DC therapy may represent a promising tool for future anti-fibrotic strategies.

Acknowledgments The authors acknowledge financial support of their work by the bilateral cooperation project #01DN1207 between Ministerio de Ciencia y Tecnología (MICYT, Argentina) and Bundesministerium für Bildung und Forschung-Deutschen Zentrum für Luft und Raumfahrt (BMBF-DLR, Germany) to S.M.B. and M.G.G. This work was supported in part by research grants from Charité Stiftung to S.M.B. and Agencia Nacional de Promoción Científica y Tecnológica PICT#2010 to G.M. and M.G.G. F.P. was recipient of a short-scholarship from the German Academic Exchange Program (DAAD), N.F. is supported by Charité Doctoral-Stipendium and I.T.-G. by the Charité Habilitation-Fellowship.

References

1. Bataller R, Brenner DA (2005) Liver fibrosis. J Clin Invest 115(2):209–218
2. Friedman SL (2008) Mechanisms of hepatic fibrogenesis. Gastroenterology 134(6):1655–1669
3. Friedman SL (2008) Hepatic stellate cells: protean, multifunctional, and enigmatic cells of the liver. Physiol Rev 88(1):125–172
4. Duffield JS, Forbes SJ, Constandinou CM, Clay S, Partolina M, Vuthoori S, Wu S, Lang R, Iredale JP (2005) Selective depletion of macrophages reveals distinct, opposing roles during liver injury and repair. J Clin Invest 115(1):56–65
5. Stauffer JK, Scarzello AJ, Jiang Q, Wiltrout RH (2012) Chronic inflammation, immune escape, and oncogenesis in the liver: a unique neighborhood for novel intersections. Hepatology 56(4):1567–1574
6. Park O, Jeong WI, Wang L, Wang H, Lian ZX, Gershwin ME, Gao B (2009) Diverse roles of invariant natural killer T cells in liver injury and fibrosis induced by carbon tetrachloride. Hepatology 49(5):1683–1694
7. Safadi R, Ohta M, Alvarez CE, Fiel MI, Bansal M, Mehal WZ, Friedman SL (2004) Immune stimulation of hepatic fibrogenesis by CD8 cells and attenuation by transgenic interleukin-10 from hepatocytes. Gastroenterology 127(3):870–882
8. Radaeva S, Sun R, Jaruga B, Nguyen VT, Tian Z, Gao B (2006) Natural killer cells ameliorate liver fibrosis by killing activated stellate cells in NKG2D-dependent and tumor necrosis factor-related apoptosis-inducing ligand-dependent manners. Gastroenterology 130(2):435–452
9. Palucka K, Banchereau J (2012) Cancer immunotherapy via dendritic cells. Nat Rev Cancer 12(4):265–277
10. Steinman RM, Banchereau J (2007) Taking dendritic cells into medicine. Nature 449(7161):419–426
11. Bleier JI, Katz SC, Chaudhry UI, Pillarisetty VG, Kingham TP 3rd, Shah AB, Raab JR, DeMatteo RP (2006) Biliary obstruction

selectively expands and activates liver myeloid dendritic cells. J Immunol 176(12):7189–7195
12. Natarajan S, Thomson AW (2010) Tolerogenic dendritic cells and myeloid-derived suppressor cells: potential for regulation and therapy of liver auto- and alloimmunity. Immunobiology 215 (9–10):698–703
13. Watanabe T, Katsukura H, Chiba T, Kita T, Wakatsuki Y (2007) Periportal and sinusoidal liver dendritic cells suppressing T helper type 1-mediated hepatitis. Gut 56(10):1445–1451
14. Connolly MK, Bedrosian AS, Mallen-St Clair J, Mitchell AP, Ibrahim J, Stroud A, Pachter HL, Bar-Sagi D, Frey AB, Miller G (2009) In liver fibrosis, dendritic cells govern hepatic inflammation in mice via TNF-alpha. J Clin Invest 119(11):3213–3225
15. Jiao J, Sastre D, Fiel MI, Lee UE, Ghiassi-Nejad Z, Ginhoux F, Vivier E, Friedman SL, Merad M, Aloman C (2012) Dendritic cell regulation of carbon tetrachloride-induced murine liver fibrosis regression. Hepatology 55(1):244–255
16. Corpechot C, Barbu V, Wendum D, Kinnman N, Rey C, Poupon R, Housset C, Rosmorduc O (2002) Hypoxia-induced VEGF and collagen I expressions are associated with angiogenesis and fibrogenesis in experimental cirrhosis. Hepatology 35(5):1010–1021
17. Rosmorduc O, Wendum D, Corpechot C, Galy B, Sebbagh N, Raleigh J, Housset C, Poupon R (1999) Hepatocellular hypoxia-induced vascular endothelial growth factor expression and angiogenesis in experimental biliary cirrhosis. Am J Pathol 155(4): 1065–1073
18. Yu C, Wang F, Jin C, Huang X, Miller DL, Basilico C, McKeehan WL (2003) Role of fibroblast growth factor type 1 and 2 in carbon tetrachloride-induced hepatic injury and fibrogenesis. Am J Pathol 163(4):1653–1662
19. Forsythe JA, Jiang BH, Iyer NV, Agani F, Leung SW, Koos RD, Semenza GL (1996) Activation of vascular endothelial growth factor gene transcription by hypoxia-inducible factor 1. Mol Cell Biol 16(9):4604–4613
20. Yoshiji H, Kuriyama S, Yoshii J, Ikenaka Y, Noguchi R, Hicklin DJ, Wu Y, Yanase K, Namisaki T, Yamazaki M, Tsujinoue H, Imazu H, Masaki T, Fukui H (2003) Vascular endothelial growth factor and receptor interaction is a prerequisite for murine hepatic fibrogenesis. Gut 52(9):1347–1354
21. Fainaru O, Almog N, Yung CW, Nakai K, Montoya-Zavala M, Abdollahi A, D'Amato R, Ingber DE (2010) Tumor growth and angiogenesis are dependent on the presence of immature dendritic cells. FASEB J 24(5):1411–1418
22. Sozzani S, Rusnati M, Riboldi E, Mitola S, Presta M (2007) Dendritic cell-endothelial cell cross-talk in angiogenesis. Trends Immunol 28(9):385–392
23. Jung S, Unutmaz D, Wong P, Sano G, De los Santos K, Sparwasser T, Wu S, Vuthoori S, Ko K, Zavala F, Pamer EG, Littman DR, Lang RA (2002) In vivo depletion of CD11c(+) dendritic cells abrogates priming of CD8(+) T cells by exogenous cell-associated antigens. Immunity 17(2):211–220
24. Thomas JA, Pope C, Wojtacha D, Robson AJ, Gordon-Walker TT, Hartland S, Ramachandran P, Van Deemter M, Hume DA, Iredale JP, Forbes SJ (2011) Macrophage therapy for murine liver fibrosis recruits host effector cells improving fibrosis, regeneration, and function. Hepatology 53(6):2003–2015
25. Alaniz L, Rizzo M, Malvicini M, Jaunarena J, Avella D, Atorrasagasti C, Aquino JB, Garcia M, Matar P, Silva M, Mazzolini G (2009) Low molecular weight hyaluronan inhibits colorectal carcinoma growth by decreasing tumor cell proliferation and stimulating immune response. Cancer Lett 278(1):9–16
26. Laskarin G, Kammerer U, Rukavina D, Thomson AW, Fernandez N, Blois SM (2007) Antigen-presenting cells and materno-fetal tolerance: an emerging role for dendritic cells. Am J Reprod Immunol 58(3):255–267
27. Webster B, Ekland EH, Agle LM, Chyou S, Ruggieri R, Lu TT (2006) Regulation of lymph node vascular growth by dendritic cells. J Exp Med 203(8):1903–1913
28. Curiel TJ, Cheng P, Mottram P, Alvarez X, Moons L, Evdemon-Hogan M, Wei S, Zou L, Kryczek I, Hoyle G, Lackner A, Carmeliet P, Zou W (2004) Dendritic cell subsets differentially regulate angiogenesis in human ovarian cancer. Cancer Res 64(16):5535–5538
29. Conejo-Garcia JR, Benencia F, Courreges MC, Kang E, Mohamed-Hadley A, Buckanovich RJ, Holtz DO, Jenkins A, Na H, Zhang L, Wagner DS, Katsaros D, Caroll R, Coukos G (2004) Tumor-infiltrating dendritic cell precursors recruited by a beta-defensin contribute to vasculogenesis under the influence of Vegf-A. Nat Med 10(9):950–958
30. Fainaru O, Adini A, Benny O, Adini I, Short S, Bazinet L, Nakai K, Pravda E, Hornstein MD, D'Amato RJ, Folkman J (2008) Dendritic cells support angiogenesis and promote lesion growth in a murine model of endometriosis. FASEB J 22(2):522–529
31. Grunewald M, Avraham I, Dor Y, Bachar-Lustig E, Itin A, Jung S, Chimenti S, Landsman L, Abramovitch R, Keshet E (2006) VEGF-induced adult neovascularization: recruitment, retention, and role of accessory cells. Cell 124(1):175–189
32. Sugimoto H, Hamano Y, Charytan D, Cosgrove D, Kieran M, Sudhakar A, Kalluri R (2003) Neutralization of circulating vascular endothelial growth factor (VEGF) by anti-VEGF antibodies and soluble VEGF receptor 1 (sFlt-1) induces proteinuria. J Biol Chem 278(15):12605–12608
33. Mahasreshti PJ, Kataram M, Wang MH, Stockard CR, Grizzle WE, Carey D, Siegal GP, Haisma HJ, Alvarez RD, Curiel DT (2003) Intravenous delivery of adenovirus-mediated soluble FLT-1 results in liver toxicity. Clin Cancer Res 9(7):2701–2710
34. Sahin H, Borkham-Kamphorst E, Kuppe C, Zaldivar MM, Grouls C, Al-samman M, Nellen A, Schmitz P, Heinrichs D, Berres ML, Doleschel D, Scholten D, Weiskirchen R, Moeller MJ, Kiessling F, Trautwein C, Wasmuth HE (2012) Chemokine Cxcl9 attenuates liver fibrosis-associated angiogenesis in mice. Hepatology 55(5):1610–1619
35. Lee JS, Semela D, Iredale J, Shah VH (2007) Sinusoidal remodeling and angiogenesis: a new function for the liver-specific pericyte? Hepatology 45(3):817–825
36. Taura K, De Minicis S, Seki E, Hatano E, Iwaisako K, Osterreicher CH, Kodama Y, Miura K, Ikai I, Uemoto S, Brenner DA (2008) Hepatic stellate cells secrete angiopoietin 1 that induces angiogenesis in liver fibrosis. Gastroenterology 135(5):1729–1738
37. Sanz-Cameno P, Trapero-Marugan M, Chaparro M, Jones EA, Moreno-Otero R (2010) Angiogenesis: from chronic liver inflammation to hepatocellular carcinoma. J Oncol 2010:272170
38. Wald O, Pappo O, Safadi R, Dagan-Berger M, Beider K, Wald H, Franitza S, Weiss I, Avniel S, Boaz P, Hanna J, Zamir G, Eid A, Mandelboim O, Spengler U, Galun E, Peled A (2004) Involvement of the CXCL12/CXCR4 pathway in the advanced liver disease that is associated with hepatitis C virus or hepatitis B virus. Eur J Immunol 34(4):1164–1174